Journal of Saudi Chemical Society (2017) 21, S293–S298

King Saud University

Journal of Saudi Chemical Society

www.ksu.edu.sa
www.sciencedirect.com

ORIGINAL ARTICLE

Sacha inchi (*Plukenetia volubilis* L.) shell biomass for synthesis of silver nanocatalyst

Brajesh Kumar *, Kumari Smita, Luis Cumbal *, Alexis Debut

Centro de Nanociencia y Nanotecnologia, Universidad de las Fuerzas Armadas - ESPE, Av. Gral. Rumiñahui s/n, Sangolqui, P.O. Box 171-5-231B, Ecuador

Received 14 February 2014; revised 10 March 2014; accepted 12 March 2014
Available online 27 March 2014

KEYWORDS

Nanostructures;
Biomaterials;
Nanocatalyst synthesis;
Fourier transform infrared spectroscopy;
Electron microscopy

Abstract This article describes a new approach for synthesis of silver nanostructured particles by using a Sacha inchi shell biomass (SISB). Sacha inchi shell biomass should be considered as an important source of phytochemicals for the synthesis and stabilization of silver nanoparticles (AgNPs). The characterization of AgNPs was performed by UV–vis spectroscopy, Transmission Electron Microscopy and Selected Area Electron Diffraction, indicating that AgNps were synthesized successfully with an average size of 7.2 nm. Infrared spectrum measurements were carried out to hypothesize the possible biomolecules responsible for stabilization and capping of the silver nanoparticles. Then, AgNps were used as a catalyst in the presence of sunlight for the removal of methyl orange dye (MO, anionic dye) from aqueous solution. The results implied AgNps to be effective photocatalyst for the decomposition of MO (~60%, pH 2.0) from aqueous solution.

1. Introduction

Silver nanoparticles (AgNps) are important materials that have been studied extensively in the recent years. They can be synthesized by several physical, chemical and biological methods [1–3]. Such nanoparticles possess unique electrical, optical as well as biological properties and are thus applied in catalysis, biosensing, imaging, drug delivery, nanodevice fabrication, medicine and antimicrobial [1,4–6]. In the past few years, there has been increasing interest in the synthesis of AgNps using biological systems, including bacteria, fungi and algae have become a cost efficient alternative to conventional physical and chemical method [7–9]. The use of soluble biopolymers as soft templates for directing crystal growth and controlling self-assembly of inorganic nanoparticles has also emerged as an important technique [10]. It was found that the large number of amine, hydroxyl and carboxylic groups on the biopolymers facilitates the formation of complexes of silver ions [11]. Subsequently, these silver ions oxidize the hydroxyl groups to carbonyl groups and carboxyl groups, while the silver ions are reduced to elemental silver. Further these metallic NPs are probably capped and stabilized by the polysaccharides. So, the bio-inspired synthesis of AgNPs has become a hot area in recent decades.

Literature survey has shown that very few naturally available agricultural wastes have been investigated for the

* Corresponding authors.
E-mail addresses: krmbraj@gmail.com (B. Kumar), lhcumbal@espe.edu.ec (L. Cumbal).
Peer review under responsibility of King Saud University.

ELSEVIER Production and hosting by Elsevier

http://dx.doi.org/10.1016/j.jscs.2014.03.005

synthesis of AgNps [12]. Thus, an efficient reuse of these wastes is of great importance, not only for minimizing the environmental impact, but also for obtaining a higher profit. A classical example of such an abundantly available natural material is the Sacha inchi shell biomass (SISB). Sacha inch is a promising crop (*Plukenetia volubilis* L.) which produces star-shaped green fruits, which yield edible dark brown seeds, very rich in oil (35–60%), proteins (27%) and contain heat-labile substances with a bitter taste [13]. It is also known as the Inca peanut, is a perennial, oleaginous plant of the Euphorbiaceae family, native from the rain forest of the Andean region of South America. The plant was known by the natives of the area for thousands of years as witnessed by several representatives reported on vessels found in Incas' tombs [14]. Chancas Indians and other tribal groups of the region extract oil from the seeds, which is used for the preparation of various meals. Roasted seeds and cooked leaves are also an important component of their diets. Thus, the utilization of these crops in industrial processes for the production of high performance materials, could be an additional source of revenue for farmers and also help in agro-industry diversification by providing a non-food-based market for agro-wastes. To the best of our knowledge, no papers have reported for the synthesis of stabilized nanoparticles using SISB. We hypothesized that SISB may be rich in biopolymers such as lignin, hemicellulose and pectins that could be used in the synthesis and stabilization of AgNps.

The aim of this present work was to synthesize, stabilize and characterize the AgNps using SISB extract; and also utilized nanoparticles as catalyst for remediation of methyl orange (MO). MO is one of the well-known acidic/anionic dyes, with IUPAC name of sodium 4-[(4-dimethylamino) phenyldiazenyl] benzene sulfonate. It has been widely used in textile, printing, paper, food, and pharmaceutical industries and research laboratories. Azo dyes are well known carcinogenic organic substances. Like many other dyes of its class, MO inadvertently enters the body through ingestion, metabolizes into aromatic amines by intestinal microorganisms [15].

2. Experimental

2.1. Materials

Silver nitrate (99.0%) and methyl orange (99.5%) were purchased from the Spectrum (USA). Millipore Milli-Q water was used in all experiments. About 50 g SISB fibers were chopped into mesh size 150–250. The chopped SISB fibers (5.0 g) were soaked in Milli Q water (100 mL) overnight in a clean environment. The brown color SISB extract was filtered by use of a muslin cloth, and the filtrate was used for the synthesis of stabilized nanoparticles.

2.2. Synthesis of silver nanoparticles

For the synthesis of AgNps, 10 mL silver nitrate solution (1 mM) was treated with 1 mL of the SISB extract at different pHs (7–12). The reaction mixture was exposed to indirect sunlight and kept at room temperature (21–23 °C). Based on the best results obtained at pH 12, we performed other characterization.

2.3. Characterization of silver nanoparticles

The synthesized AgNps were characterized with the help of a UV–vis spectrophotometer (Thermospectronic, GENESYS™ 8). Size of nanoparticles was analyzed by using Dynamic Light Scattering (DLS) instrumentation (HORIBA LB-550). Transmission Electron Microscopy (TEM) and Selected Area Electron Diffraction (SAED) were performed in support film of 2% polyvinyl formal solution stabilized with carbon. Briefly, TEM and SAED images were recorded digitally (FEI Tecnai G2 Spirit Twin). Fourier transform infrared (FTIR-ATR) spectra were recorded on a Perkin Elmer (Spectrum Two) spectrophotometer to hypothesize functional groups involved in the synthesis of starches AgNps.

2.4. Decomposition of dyes

Three separate sets of experiments were performed for studying the decomposition of MO by taking different pHs 5.6, 3.0 and 2.0. In set 1, 2 mL MO (64 mg/L), and 2 mL H_2O were mixed in a vial and kept in the sunlight. In set 2, 2 mL MO, 0.2 mL SISB extract and 1.8 mL H_2O were added and kept in the sunlight. In set 3, the synthesized AgNp catalyst was used; 2 mL MO, 0.2 mL SISB extract, 1.0 mL AgNp catalyst and 0.8 mL H_2O were mixed and kept in the sunlight. All three sets of reactions were observed after 30 min. The rate of dye decomposition was monitored by taking 4 mL samples from each set and recording the UV–vis spectra using UV–vis spectrophotometer (Thermo spectronic, GENESYS^{TM} 8) at the wavelength of maximum absorption of MO (λ_{max} = 464 nm). Typically the catalytic activity of AgNps was observed best for degradation of MO at pH 2 in the presence of sunlight.

3. Results and discussion

3.1. Visual and UV–vis studies

The most widely used method for the synthesis of metallic nanoparticles is wet-chemical procedures, which involves growing nanoparticles in a liquid medium containing various reactants, in particular reducing agents. The advantage of this method is the low cost for high volume synthesis, but the major drawbacks of this method include contamination from precursor chemicals and the use of toxic solvents, which shows adverse effects on the environment and human health [16]. Fig. 1(a and b) shows the visual effect of $AgNO_3$ before and after treatment to SISB extract. For the synthesis of AgNps, 1 mL of SISB extract was added to 10 mL of $AgNO_3$ (pH 12) and kept for a period of 30 min at room temperature. Change of color from colorless to yellow color, shows the formation of nanoparticles and the absorption maximum at 420 nm decreased steadily as a function of reaction time (Fig. 2). This is attributed to a resonance in the collective motion of the conduction electrons. This phenomenon is called the localized surface plasmon resonance (LSPR) of AgNps in the visible region [17], which clearly indicates the preliminary synthesis of AgNps (Fig. 1b). The absorption band depends on the shape, size and the surrounding medium of the particle [18]. For comparison purpose, without treatment of $AgNO_3$ with SISB extract, no maximum absorbance was observed

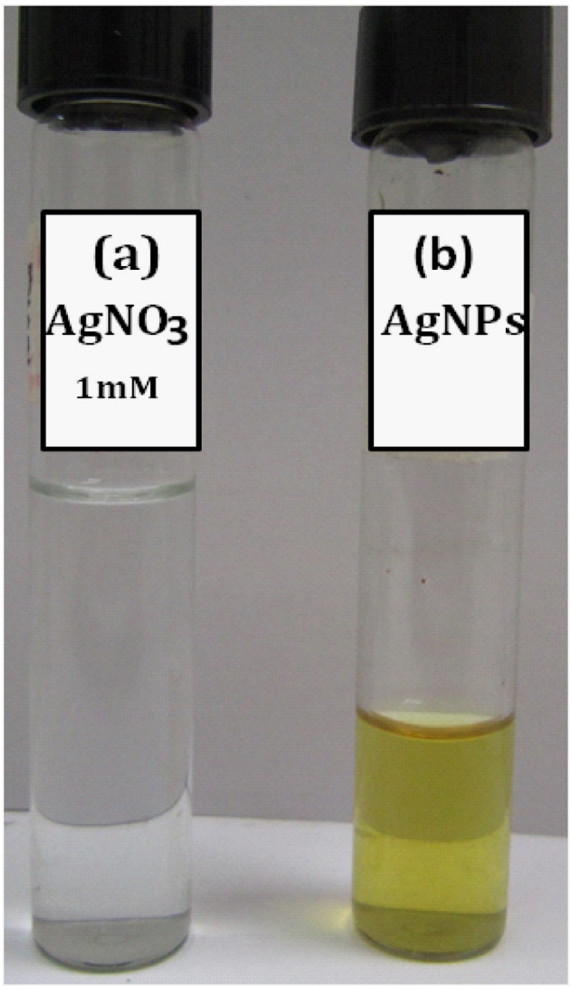

Figure 1 (a) 1 mM $AgNO_3$ solution and (b) AgNps.

between 400 and 450 mm. It indicates that, SISB extract, bound with $AgNO_3$ and was the possible reducing agent for the synthesis of AgNps. The bioreduction of silver could occur through the oxidation of hydroxyl to carbonyl groups as shown in Eq. (1):

$$AgNO_3 + R\text{–}OH \rightarrow Ag^0 + R{=}O + NO_3^- + H^+ \quad (1)$$

3.2. DLS studies

In order to determine the particle size distribution of AgNps in solution, DLS measurements were carried out after 6 days of reaction time. The qualitative DLS size distribution image of AgNps is shown in Fig. 3. The average particle sizes of AgNps are 7.2 nm and standard deviation, σ = 1.7 nm, respectively. From the results of the above study, it could be inferred that the formation of AgNps is highly stable.

3.3. TEM and SAED studies

The TEM images of stable AgNps and the SAED pattern recorded after 6 days of reaction time are depicted in Fig. 4(a–c). From the images, it can be seen that the AgNps were spherical in shape, having an average size of 2–15 nm. Generally,

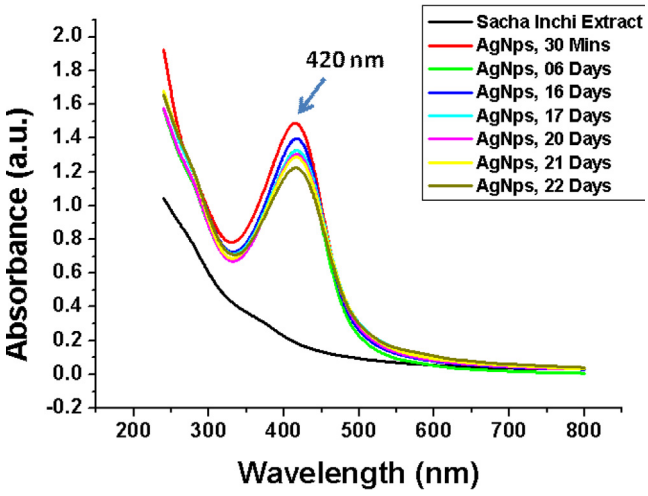

Figure 2 U.V.-vis graph for AgNps synthesized by using SISB extract.

nanoparticles were prepared in a solution phase, the solute particles need to overcome a large surface area barrier and tend to have a spherical shape because this shape has the smallest surface area relative to objects of other shapes. The SAED (Fig. 4d) pattern reveals that the synthesized AgNps are partially crystalline and are capped with phytoconstituents of the extract. The exact mechanism of reducing nature of SISB extract is unclear; to our knowledge it may be that SISB extract rich in polymers such as lignin, hemicellulose and pectins could be used in the synthesis of silver nanoparticles.

3.4. FTIR studies

FTIR spectroscopy from the absorption of IR radiation through modes of vibration is a useful technique to study the interaction of AgNPs with SISB. The peaks obtained were compared with SISB, and a slight shift was observed in the purified AgNPs. Fig. 5a shows FTIR spectrum of SISB broad peak at 3286 cm^{-1} is indicative of the existence of bounded –NH_2 and O–H bond stretch groups of macromolecular association (cellulose, pectin, etc.). The bands at 1597 cm^{-1} are observed as amide and arise due to carbonyl stretch and –NH stretch vibrations in the amide linkages of the SISB correspondingly. The band at 1242 cm^{-1} related to SO_3 stretching could be observed in the FTIR spectra of SISB. The FTIR spectroscopic study has confirmed (Fig. 5b) that the –NH group (3330 cm^{-1}) and SO_3 (1263 cm^{-1}) of SISB have stronger ability to bind metal [19]. So, the polysaccharide most possibly might have formed a layer on the AgNPs (i.e., biological reducing and capping) which also prevents agglomeration of the particles, and thus the nanoparticles are stabilized in the medium.

3.5. MO decomposition kinetics and its measurements

Besides the optical properties, AgNps have excellent catalytic activity. Generally it is accepted that chemistry changes with size [20]. The role of metal nanoparticle as an electron transfer catalyst is thus expected to vary with size. The performance of the AgNps was examined as a function of the operating

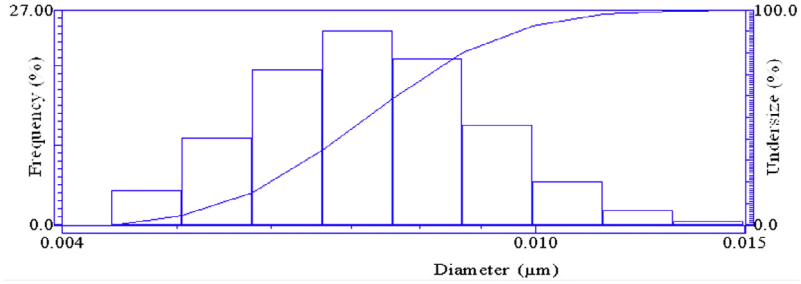

Figure 3 Histogram showing the size distribution of AgNps (Median = 7.2 nm/0.0072 µm, Mean = 7.4 nm/0.0074 µm and σ = 1.7 nm/0.0017 µm).

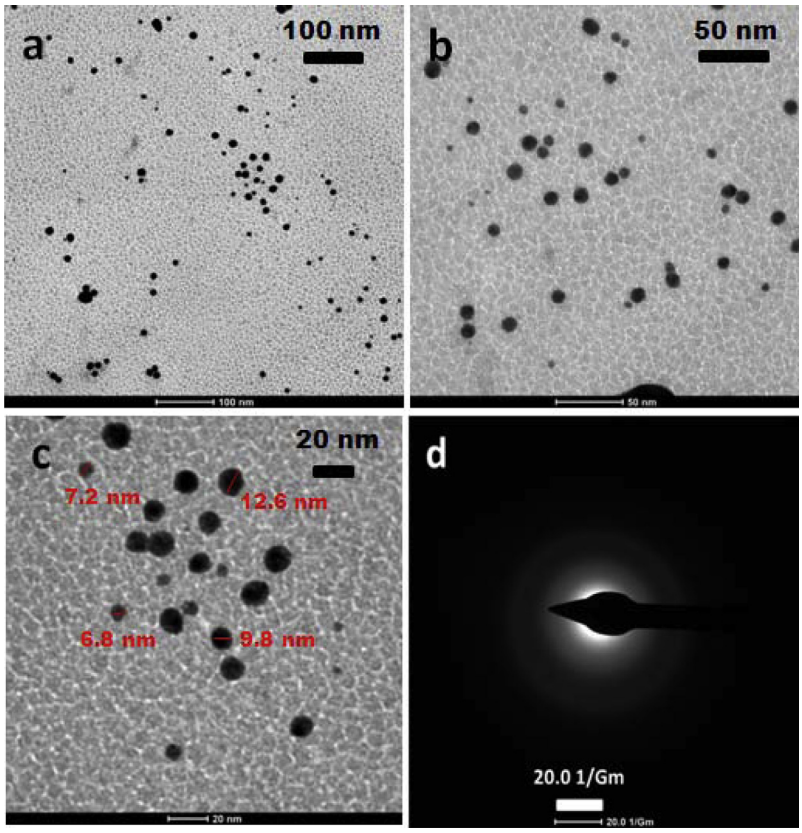

Figure 4 TEM images of AgNps (a–c) derived from SISB extract and SAED pattern (d).

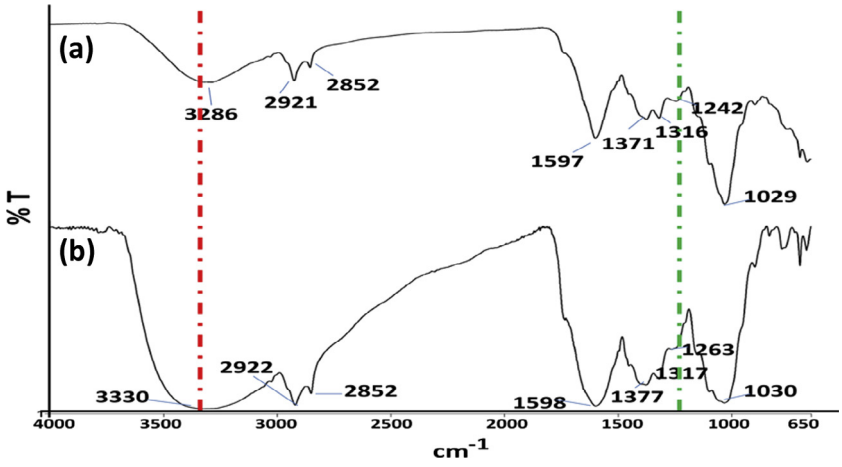

Figure 5 FTIR spectra of (a) SISB and (b) synthesized AgNPs.

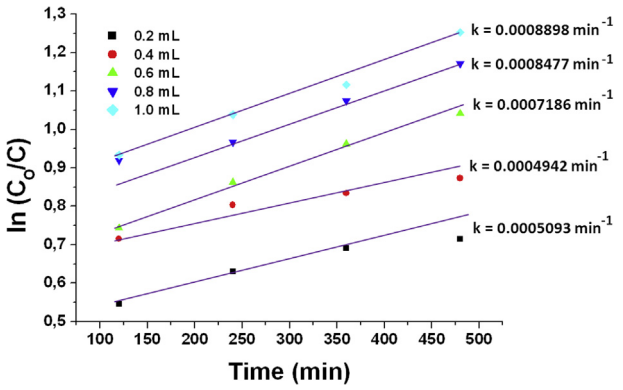

Figure 6 Kinetics of photocatalytic degradation of MO, Plot of $\ln(C_0/C)$ vs irradiation time.

different pH conditions. MO molecules are predominantly present as monovalent anions (pKa = 3.46). The color of an azo dye is the result of the interaction between an azo function (—N═N—) and two aromatic species: the dyes carry an acceptor group which is an aromatic nucleus frequently containing a chromophoric group, e.g. $-SO_3^-$, and a donor group, e.g. an aromatic nucleus containing an auxochromic group such as alkyl side chains, or the OH group [21]. The Kinetic study model [22] can be used to describe the relationship between the rates of the photocatalytic degradation of MO dye in the presence of AgNps by using the following Eq. (2):

$$\ln(C_0/C) = kKt = Kt \quad (2)$$

where, K is the adsorption coefficient of the reactant on AgNPs, k is the reaction rate constant and C is the concentration of the reactant at any time t, C_0 is initial concentration, k = kK is the pseudo first order reaction rate constant. Plotting $\ln(C_0/C)$] versus the corresponding irradiation time (min) yields a linear relationship as shown in Fig. 6. The rate constant of photocatalytic degradation of MO dye was investigated by using different initial concentrations (0.2, 0.4, 0.6, 0.8 and 1.0 mL) of AgNps. The rate constant was evaluated from the slope of the straight line from Fig. 6. By increasing the concentration of AgNPs the surface area of the active site of Ag nanocatalyst was increased. So, the rate of the reaction

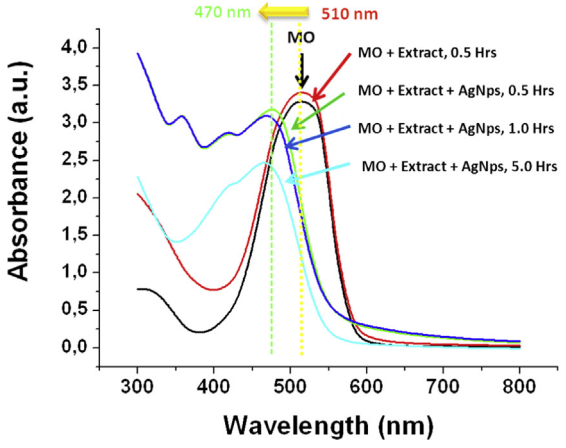

Figure 7 Photocatalytic effect of AgNps for remediation of MO at pH 2.0.

was increased gradually. The rate constant was found to be highest (0.0008898 min^{-1}), when 1 mL of AgNps solution was used in the photocatalytic degradation reaction.

Fig. 7 shows the UV–vis absorption spectra of MO decomposition by SISB extract in the presence of AgNps at pH 2. The spectra show that SISB extract alone does not cause any appreciable change in the decomposition of the MO. AgNp catalyst and SISB extracts increased the rate of decomposition of MO, as is an apparent decrease and shift of absorbance from 510 nm to 470 nm. The decrease is also meaningful with respect to the nitrogen-to-nitrogen double bond (—N═N—) of the azo dyes, as the most active site for oxidative attack. Decrease in the absorption intensity of the band at λ_{max} during the irradiation also expresses the loss of conjugation, e.g. especially the cleavage near the azo bond of the organic molecule. In this study, the use of UV radiation of sunlight for the photocatalytic degradation of MO in the presence of AgNPs was investigated. When the reaction is conducted under sunlight using glass tubes (glass is opaque to UV light), the degradation activity increased drastically.

The average decomposition in terms of the percentage of MO in solution was calculated using the following Eq. (3):

$$\eta = [A_0 - A_t/A_0] \times 100\% \quad (3)$$

where η is the rate of decomposition of MO in terms of percentage, A_0 is the initial absorbance of MO solution and A_t is the absorbance of the dyes at time t [23]. The experimental evidence shows a strong effect of the pH 2 for maximum removal of MO (~60%, 5 h, 64 mg/L) from aquatic systems.

4. Conclusion

The study indicated that cheaply available Sacha inchi shell biomass (SISB) can be used for the biosynthesis of AgNps and AgNPs acts as a photocatalyst of remediation of methyl orange (MO). Activity and rate of the reaction increase with increasing the concentration of nanoparticles. The AgNps synthesized were predominantly spherical with an average size of 7.2 nm and S.D = 1.7 nm. SISB mediated AgNps were demonstrated to be a simple, low-cost and ecofriendly method and can be used as an alternative agent for ~60% removal of the anionic dye MO from aqueous solutions, without any laborious pre-treatment. SISB mediated synthesis of AgNps is a very promising nanomaterial for the removal of MO.

Acknowledgments

This scientific work has been funded by the Prometeo Project of the Ministry of Higher Education, Technology and Innovation (SENESCYT), Ecuador. We thank Mr. Abraham Rodolfo Sanchez Piñuela for providing Sacha inchi shell biomass (SISB) as gift for performing experiments.

References

[1] L.S. Nair, C.T. Laurencin, Silver nanoparticles: synthesis and therapeutic applications, J. Biomed. Nanotechnol. 3 (2007) 301–316.

[2] Y. Zhang, H. Peng, W. Huang, Y. Zhou, D. Yan, Facile preparation and characterization of highly antimicrobial colloid Ag or Au nanoparticles, Colloids Interface Sci. 325 (2008) 371–376.

[3] V.K. Sharma, R.A. Yngard, Y. Lin, Silver nanoparticles: green synthesis and their antimicrobial activities, Adv. Colloid Interface Sci. 145 (2009) 83–96.
[4] K.S. Lee, M.A. El-Sayed, Gold and silver nanoparticles in sensing and imaging: sensitivity of plasmon response to size, shape, and metal composition, J Phys. Chem. B 110 (2006) 19220–19225.
[5] P.K. Jain, X. Huang, I.H. El-Sayed, M.A. El-Sayed, Noble metals on the nanoscale: optical and photothermal properties and some applications in imaging, sensing, biology, and medicine, Acc. Chem. Res. 41 (2008) 1578–1586.
[6] O. Choi, K.K. Deng, N.J. Kim, L. Ross Jr., R.Y. Surampalli, Z. Hu, The inhibitory effects of silver nanoparticles, silver ions, and silver chloride colloids on microbial growth, Water Res. 42 (2008) 3066–3074.
[7] N. Saifuddin, C.W. Wong, A.A.N. Yasumira, Rapid biosynthesis of silver nanoparticles using culture supernatant of bacteria with microwave irradiation, E J. Chem. 6 (2009) 61–70.
[8] D.S. Balaji, S. Basavaraja, R. Deshpande, D.B. Mahesh, B.K. Prabhakar, A. Venkataraman, Extracellular biosynthesis of functionalized silver nanoparticles by strains of *Cladosporium cladosporioides* fungus, Colloids Surfaces B 68 (2009) 88–92.
[9] J. Xie, J.Y. Lee, D.I.C. Wang, Y.P. Ting, Silver nanoplates: from biological to biomimetic synthesis, ACS Nano 1 (2007) 429–439.
[10] S.H. Yu, S.F. Chen, Recent advances on polymer directed crystal growth and mediated self-assembly of nanoparticles, Curr. Nanosci. 2 (2006) 81–95.
[11] (a) N. Vigneshwaran, R.P. Nachane, R.H. Balasubramanya, P.V. Varadarajan, A novel one-pot 'green' synthesis of stable silver nanoparticles using soluble starch, Carbohydr. Res. 341 (2012) 2012–2018;
(b) B. Kumar, K. Smita, L. Cumbal, A. Debut, R.N. Pathak, Sonochemical synthesis of silver nanoparticles using starch: A comparison, Bioinorg. Chem. Appl. 10 (2014). Article ID 784268.
[12] A. Banker, B. Joshi, A.R. Kumar, S. Zinjarde, Banana peel extract mediated novel route for the synthesis of silver nanoparticles, Colloids Surf. A Physicochem. Eng. Aspects 368 (2010) 58–63.
[13] C. Fanali, L. Dugo, F. Cacciola, M. Beccaria, S. Grasso, M. Dacha, P. Dugo, L. Mondello, Chemical Characterization of Sacha Inchi (*Plukenetia volubilis* L.) Oil, J. Agric. Food Chem. 59 (2010) 13043–13049.
[14] M.D. Guillen, A. Ruiz, N. Cabo, R. Chirinos, G. Pascual, Characterization of Sacha inchi (*Plukenetia volubilis* L.) oil by FTIR spectroscopy and H NMR. Comparison with linseed oil, J. Am. Oil Chem. Soc. 80 (2003) 755–762.
[15] A. Mittal, A. Malviya, D. Kaur, J. Mittal, L. Kurup, Studies on the adsorption kinetics and isotherms for the removal and recovery of methyl orange from wastewaters using waste materials, J. Hazard. Mater. 148 (2007) 229–240.
[16] K.N. Thakkar, S.S. Mhatre, R.Y. Parikh, Biological synthesis of metallic nanoparticles, Nanomedicine 6 (2010) 257–262.
[17] D. Manikprabhu, K. Lingappa, Microwave assisted rapid and green synthesis of silver nanoparticles using a pigment produced by streptomyces coelicolor klmp33, Bioinorg. Chem. Appl. (2013). Article ID 341798.
[18] S. Malynych, G. Chumanov, Extinction spectra of quasispherical silver sub-micron particles, J. Quant. Spectrosc. Radiat. Transf. 106 (2007) 297–303.
[19] P.X. Sheng, Y.P. Ting, J.P. Chen, L.J. Hong, Sorption of lead, copper, cadmium, zinc, and nickel by marine algal biomass: characterization of biosorptive capacity and investigation of mechanisms, Colloid Interface Sci. 275 (2004) 131–141.
[20] N. Cheval, N. Gindy, C. Flowkes, A. Fahmi, Polyamide 66 microspheres metallised with in situ synthesised gold nanoparticles for a catalytic application, Nanoscale Res. Lett. 7 (2012) 182.
[21] N. Daneshvar, A.R. Khataee, D. Salari, A. Niaei, Photocatalytic degradation of the herbicide erioglaucine in the presence of nanosized titanium dioxide: comparison and modeling of reaction kinetics, J. Environ. Sci. Heal. B 41 (2006) 1273–1290.
[22] C. Tamuly, M. Hazarika, M. Bordoloi, M.R. Das, Photocatalytic activity of Ag nanoparticles synthesized by using *Piper pedicellatum* C.DC fruits, Mater. Lett. 1–4 (2013) 102–103.
[23] M.M. Khan, J. Lee, M.H. Cho, Au@TiO_2 nanocomposites for the catalytic degradation of methyl orange and methylene blue: An electron relay effect, J. Ind. Eng. Chem. (in press), doi: http://dx.doi.org/10.1016/j.jiec.2013.08.002.